

# Feasibility Study of Flettner Rotor Propulsion Using Numerical Analysis

<sup>1</sup>Vipin Devaraj, <sup>2</sup>Jobin Raju

<sup>1</sup>Department of Ship Technology

<sup>1</sup>Cochin University of Science and Technology, Kochi-22, India

**Abstract**—viscous flow over a rotating cylinder and Magnus effect has been subject to rigorous experiments from the end of 19th century. The lift generated by the rotating cylinder is due to differential pressure gradient. This is explained along the lines of aerofoil lift theory. The phenomenon found its application onboard ships in the form of flettner rotor in the beginning of 20th century. But cheap fossil fuels and advanced technologies in power generation left behind the possibility of a greener and efficient way of propulsion concept. This paper is an attempt to highlight applicability of flettner rotor for marine use. The shipbuilding industry is sceptic to embrace new technologies and accommodate the greener possibilities. This paper devices a methodology to conduct feasibility study of flettner rotor propulsion in merchant vessels making use of Naval Architecture concepts and numerical analysis. Numerical analysis is done to obtain the performance of flettner rotor under certain conditions of wind and rotor speed.

**Index Terms**— Flettner Rotor, STAR-CCM, Ansys, Thom disc, Cylinder, Spin Ratio

## I. INTRODUCTION

Wind is a viable source of renewable energy in both land and water. In earlier days, sails were used to harness wind energy in small boats and pleasure crafts. German engineer Antonio Flettner, in 1924, experimented with the concept of fitting a long cylinder with its ends closed in a schooner. He found that wind energy can be more effectively exploited in propelling the ship using flettner rotor. Prandtl suggested that addition of discs to the bare rotating cylinder can provide higher lift. He also found that when the rotor speed is around four times the wind speed lift coefficient more than twice that of bare cylinder was obtained. The rotating cylinders installed on the ship deck converts wind energy into thrust in a direction almost perpendicular to the wind direction. 'Buckau' the first rotor propelled ship claims to have added almost 50 percent more power to its conventional engine. The International Wind Ship Association (IWSA) and Paris Climate meetings look forward to adopting greener shipping solutions thereby reducing carbon emission.

The present study is performed on a model ship fitted with flettner rotor to analyse the possible energy savings based on lift force, propeller thrust and main engine rating. The optimization of the flettner rotor geometry is also carried out assuming constant diameter and wind speed since these parameters are constraints and location specific.

## II. LITERATURE OVERVIEW

The capability of infinite length rotating cylinders to produce aerodynamic forces was studied for the first time at the Langley NACA Laboratory by Reid [2]; he found that in particular conditions such simple devices are capable of developing very high values of the lift coefficient and of the aerodynamic efficiency (i.e., the lift-to-drag ratio). Thom [3] presented an experimental work on rotating cylinders, with emphasis on the effects of the Reynolds number (Re), surface conditions, aspect ratio, and end plates disks, describing the device in terms of lift, drag, and torque coefficients. Successively, Swanson [4] clarified the physics underpinning the FR, thus highlighting the nature of the circulation around the rotating cylinder. More recently, a comprehensive study on the functioning of FR was conducted by Da-Qing et al. [5].

This work presents a numerical study of aerodynamic performance of Flettner. Special attention is paid to the formation of vortex structures and the relationship between wake instability and fluctuation of aerodynamic loads. This paper also reports statistical expressions correlating  $CL$ .

The aerodynamic coefficients of an FR depend on various parameters (geometrical and functional). In the following subsections the most important parameters are briefly summarized.

**Spin Ratio** : The amount of aerodynamic force generated by a rotating cylinder, that is, an FR, is mainly dependent on the SR (or velocity ratio, also named  $\alpha$ ), which accounts for the angular speed  $\Omega$ , the FR diameter  $d$ , and the free stream velocity  $U$ , as shown in Figure 1. The flow phenomena around a 3D circular cylinder are rather complex and feature both tip vortices and an alternate vortex shedding between the rotor sides. Seifert [6] highlights that vortex shedding occurs for Re all the way up to at least  $8.0 \cdot 10^6$  and that the extension of the vortices depends also on the Strouhal number (St). The St represents the degree of unsteadiness of the oscillating flow past the rotating cylinder. In Mittal and Kumar [7], a detailed analysis of St Regimes for rotating cylinders is presented. Low Strouhal numbers ( $St < 10^{-4}$ ) indicate long eddy formations; hence, the flow is considered quasi-steady. According to Badalamenti and Prince [8], the shedding phenomena are also influenced by SR: small spin ratios cause long eddy formations, while higher SRs cause considerably short eddies. Thus, the Karman` vortex street is seen for  $SR \leq 2$  when large eddies are formed and shed alternately on the two sides of the cylinder. Conversely, vortex formation and shedding

can no longer be seen for  $2.0 \leq SR < 3.0$ , and for  $3.0 \leq SR < 3.5$  quasi-steady-states are observable. At  $SR = 3.5$  a second shedding mode is found.

Swanson [4] pointed out that lift and drag of a rotating cylinder at  $SR < 1.0$  show a significant dependency on  $Re$ . The effects of  $Re$  are more evident on lift at  $Re > 6 \times 10^4$ , which is also confirmed by Gowree and Prince [9]. When  $SR > 2.5$  and  $Re > 4 \times 10^4$ , drag and lift curves have a slightly growing trend for increasing  $Re$ .

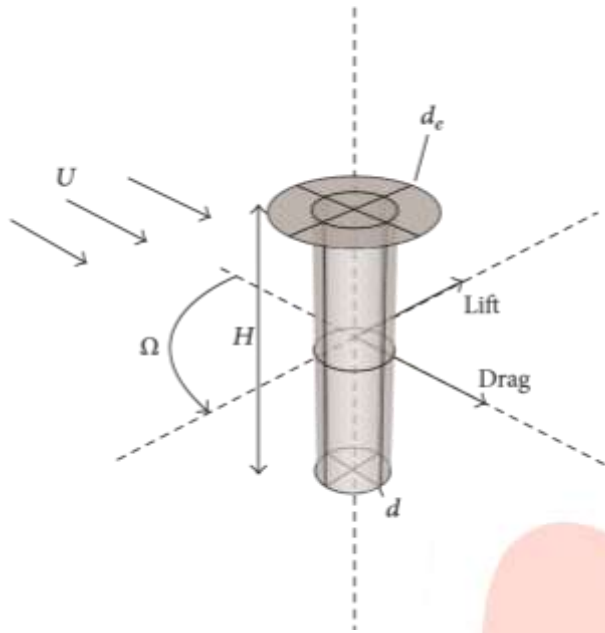


Figure 1: Sketch of Flettner Rotor with end plate and associated parameters.

**Aspect Ratio :** The main shape factor of an FR is the aspect ratio AR, which significantly influences the FR effectiveness in producing aerodynamic forces. The AR of FR device, which is the ratio between height and diameter, modifies its aerodynamic efficiency, as for higher aspect ratios the FR device behaves much like a wing, with tip vortices that take part in the lift production. An important consideration is presented by Swanson [4], who observed that the smaller the aspect ratio the smaller the maximum lift obtained and the smaller the velocity ratio at which this maximum is reached. Swanson also demonstrated that, for very high aspect ratio, the lift can reach higher values than the maximum theoretical limit predicted by Prandtl's classical theory [10]. An extensive comparison of the main data available in the literature on FR performances, both experimental and numerical ones, along with some considerations, can be found in De Marco et al.

**End Plate:** The idea of applying an end plate on FR to optimize its aerodynamic efficiency was first suggested by Prandtl [10]. The presence of an end plate modifies the 3D flow phenomena at the tip of the FR, augmenting the "effective AR" of the rotor. Thom [3] investigated the effect of large end plates with a diameter ratio  $d_e/d = 3.0$ , where  $d_e$  is the diameter of the end plate disk (Figure 2).

The FR with end plate, also called Thom disk, is able to produce almost double the lift at high velocity ratios; for example,  $SR = 2.0$ . In Badalamenti and Prince [12] it is shown that for a cylinder with  $AR = 5.1$  and diameter ratios ranging from 1.1 to 3.0, the effects of the increases  $d_e/d$  and AR are similar. Increasing the  $d_e/d$  value, a higher lift value is generated by the FR and such value occurs at higher SR as well (see Seifert [6]). Thouault et al. [13] presented a detailed analysis of the effects of end plate dimensions on the FR efficiency, based on experiments and numerical simulations.

A discussion of how the end plate size is related to SR in order to achieve optimal performances of the FR is presented by Seifert [6]. In his work Seifert observes that at low spin ratio ( $SR = 1.0$ ) smaller plates generally give lightly smaller drag; for applications at moderate spin ratio ( $1.0 < SR < 3.0$ ) larger plates are preferred, so as to delay the increase in induced drag, while, for high spin ratio applications ( $SR > 3.0$ ), smaller plates are again more desirable.



Figure 2: Estraden

**Marine Application of FR :** Concerning the use of FR for marine applications, not many research papers are available in the literature. An overview of the applications of the Magnus effect devices in the marine field is given in Morisseau [14]. The Magnus effect devices can be used as roll stabilizers, water propellers, and air generator, such as FR. Moreover this paper reports an interesting preliminary analysis of retrofitting of a single screw US Navy auxiliary ship with five FRs. More recently, in Pearson [15], a “firststage” assessment is found in practical limitations as well as negative side effects of retrofitting Flettner rotors to a ship. All these considerations are collected in order to create a software model for a preliminary analysis of the viability of retrofitting FR to a defined ship, before any progression onto analyzing specific scenario benefits or other detailed investigations. A limit of this work is in the estimation of FR performances, which are evaluated only as a function of SR. The software presented assumes a universal FR geometry, with  $de/d = 1.5$  and  $AR = 5$  (based on Prandtl’s study [10]) and evaluates  $CL$  and  $CD$  of this FR; then, the performances of FR are evaluated changing SR in the range 0.0~8.0.

Traut et al. [16] explore the potential for harnessing wind power for shipping applications. Numerical models of the two main wind power technologies, FR and towing kite, are linked with wind data along a set of five trade routes. The results of their analysis give an estimation of the average wind power contribution on a defined route. For a single FR, the delivered power is in a range between 193 and 373 kW and, for the towing kite, between 127 and 461 kW. The FR has a variability of the delivered power smaller than the towing kite, due to the different dependencies on wind speed and direction. The average power contribution coming from an FR is higher than that coming from the kite on some routes and lower on others. But an advantage of FR is that the contribution would be expected to increase almost linearly with the number of devices installed on the same ship (in this respect, a quantitative study of interference effects is lacking in the literature). For this reason, for instance, installing three FRs on a 5500 DWT (dead weight tonnage) general cargo carrier could provide, on average, more than half the power required by the main engine under typical slow steaming conditions.

#### FLETTNER ROTOR INSTALLATIONS AND REFERENCE DATA

To choose the ranges of the key parameters some constraints have been taken into account. For instance one has to consider the currently available technology as well as the practicality in marine applications. Another important factor is the vortex shedding risk (first and second mode) which depends on the mutual interaction between AR and SR. Consequently the limits of AR and SR have been identified by the analysis of some real FR installations on board.

Ship (year)	Buckau (1924)	Barbara (1926)	E-Ship 1 (2010)	Estraden (2014)
Height (m)	15.6	17	27	19
Diameter (m)	2.8	4	4	3
Aspect Ratio	5.6	4.3	6.8	6.3
Max RPM	135	150	NA	250

Table 1: Geometric and performance parameters collected from all known rotor ships

The known installations of FR and their reference data are summarized in Table 1. The first two examples, Buckau and Barbara, are not in service, while the two ships, EShip-1 and Estraden (Figure 2), are currently operated by North European owners for commercial purposes. In all of these examples a Thom disk is used and the AR are in the range 5.5~7.0. This range is taken as a reference for the investigations presented here. It is observed that the angular rotor speeds have increased over the years, thus allowing higher SR. However the SR values of interest for marine application remain in the range 1.0 to 3.0. For example,  $SR = 2.5$  is obtained for a typical relative wind velocity of 20 kn (10 m/s), a reasonable diameter of 3.0 m, and a rotation speed of 160 rpm.

#### NUMERICAL EXPERIMENTS

Systematic variations of FR configurations have been investigated by means of URANS simulations in incompressible flow. All the analyses have been performed using the commercially available computational fluid dynamics software CD Adapco STAR-CCM+ v. 8.06 and Ansys Fluent. The simulations were conducted using the same approach, such as the overset/chimera grid

technique, described in De Marco et al. [17] and in De Marco et al. [11]. The characteristics of FRs were evaluated in terms of lift and drag coefficients and aerodynamic efficiency

**Simulation Setup:** The rotating motion of the FR was simulated using the overset/chimera mesh methodology with distance-weighted interpolation method. This method, which is especially suitable for rotational movements, uses an interpolation factor inversely proportional to the distance from acceptor cell to donor cell, as indicated in CD Adapco User's Guide [18].

Hybrid mesh approach, coupling unstructured and structured mesh, has been used for all the simulations. The computational domain contains two regions the background, nonrotating, region and the overlapped, rotating, region. For the background and overlapped region, an unstructured grid approach was used, while a structured boundary layer mesh was created near the FR surface. The choice of hybrid mesh approach is justified by the fact that this is a suitable compromise between accuracy and computational effort compared with the Cartesian mesh, as shown in the 2D preliminary study reported in De Marco et al. [11]. Furthermore the grid set up allowed a non-dimensional wall distance ( $y^+$ ) value approximately equal to 1.0.

The chosen URANS-solving algorithm uses a first-order forward Euler scheme for the temporal discretization, an implicit element-based finite volume method, and a segregated flow approach with second-order upwind discretization of the convective terms. A fully turbulent approach with  $k-\omega$  Shear Stress-Transport (SST) turbulence model has been used.

It has to be noted that the simulation time step is a function of the angular speed  $\Omega$ . For the convergence of the numerical scheme, as a rule of thumb, there is a limitation on the maximum cell-based Courant-Friedrichs-Lewy (CFL) number in a time step. Therefore, the higher the angular speed, the lower the time step.

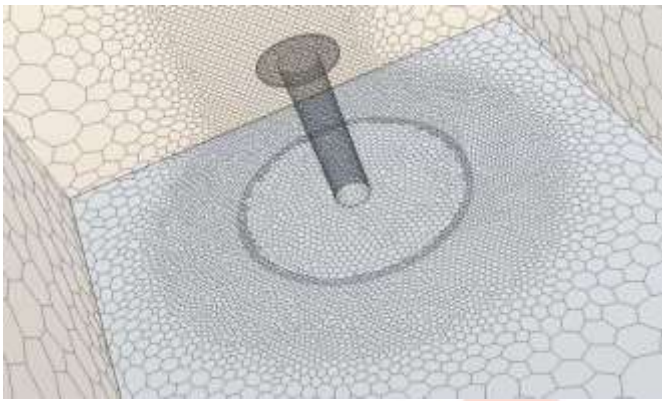


Figure 3: Geometry and hybrid mesh section

### COMPUTATIONAL DOMAIN AND BOUNDARY CONDITIONS

A box-shaped domain has been created around the cylinder geometry, as seen in Figure 4. In order to reduce the computational effort, only half the domain has been considered and a symmetry plane has been assumed, containing the cylinder axis and parallel to the free stream velocity. A velocity inlet boundary condition has been set on the front side of the domain with a prescribed velocity: this inlet velocity also has been used to control the SR of the rotor, keeping constant its angular speed  $\Omega$ . On the bottom and the top side of the domain, a symmetry boundary condition also is used. On the rear side of the domain surface, a pressure outlet

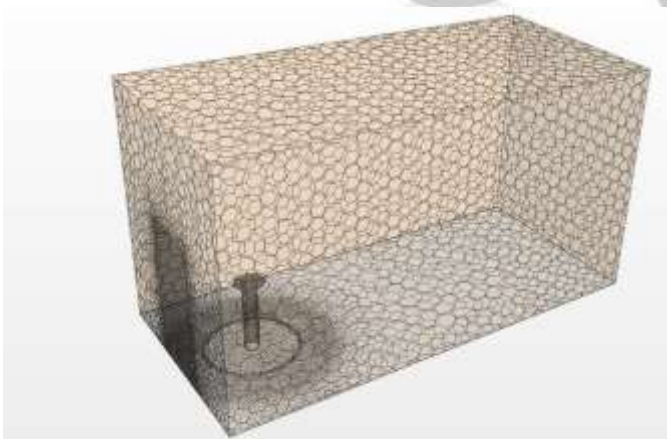


Figure 4: FR and box domain-simulation setup, The verification study has been carried out for the critical points of SR = 2.0 and SR = 2.5.

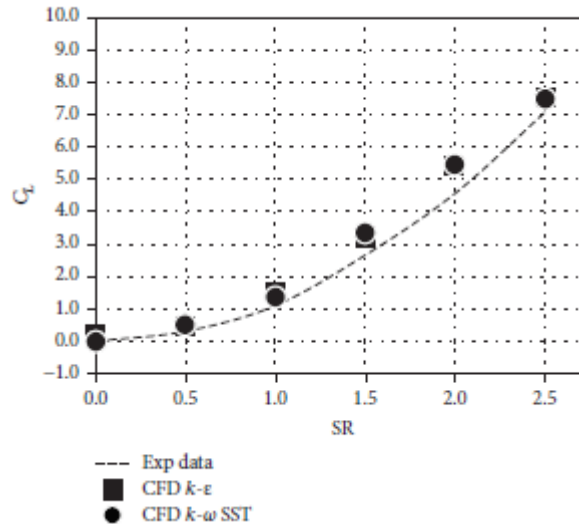
boundary condition has been imposed with a relative pressure of value 0 Pa. An axial-symmetrical zone surrounding the rotor had to be modelled, overlapping the rotating mesh (fixed with the rotor) and the underlying non-moving mesh domain. This turned out to be a necessary grid treatment for using the overset mesh methodology.



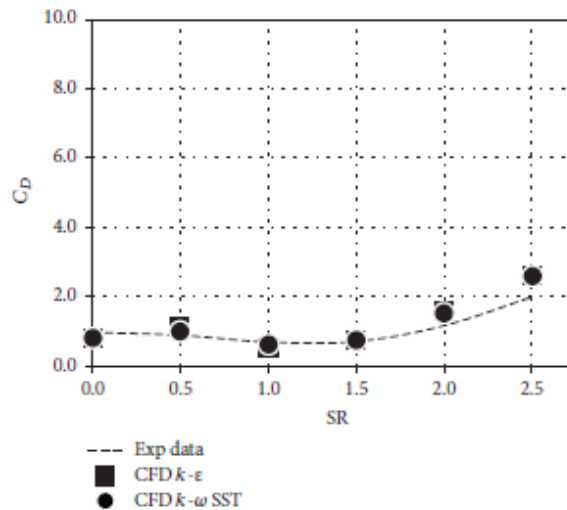
The benchmark experimental data are derived from Badalamenti and Prince [8, 12] and are related to an FR with  $AR = 5.1$  (cylinder height  $H = 0.45$  m), diameter of  $d = 0.0889$  m, and the Thom disk, on the top of this FR, with  $de = 0.1778$  m (corresponding to  $de/d = 2.0$ ).

In the CFD simulation, the boundary condition are specified in such a way that at inlet a uniform velocity is prescribed & on the surface of the cylinder a non-slip wall is arranged, also the curvature of cylinder is provided with moving walls. Various other aspects & boundary conditions were well defined to get accurate results. The simulation is computed as laminar boundary layer flow.

## RESULTS



Graph 1: Comparison of simulation results: Spin ratio v/s lift coefficient



Graph 2: Comparison of simulation results: Spin ratio v/s drag coefficient

The following  $C_d$  and  $C_l$  values were obtained from the simulation. The trend is clear from the graph that, the coefficient of lift,  $C_l$  increases as the Spin ratio (SR) increases.

The simulation results are also in agreement with the experimental results. This paves way for an optimization process of the Flettner rotor using the various aspects like Spin ratio, which can lead to a proper marine propulsive use of the rotor.

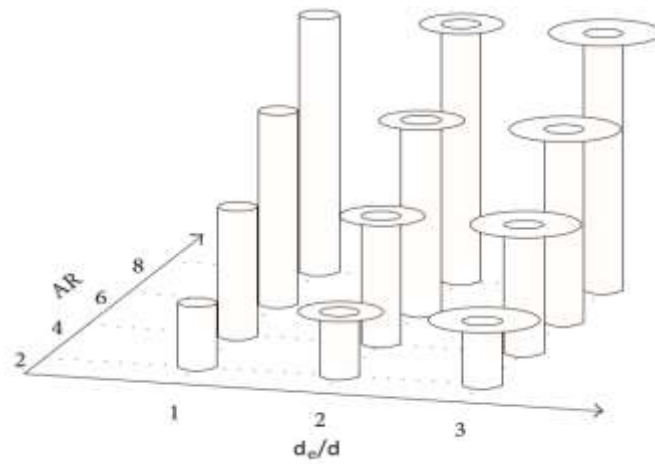


Figure 5 : Optimization process of the Flettner rotor

The perfect aspect ratios, spin and velocity ratios can cumulatively lead to the perfect FR for the desired marine route.

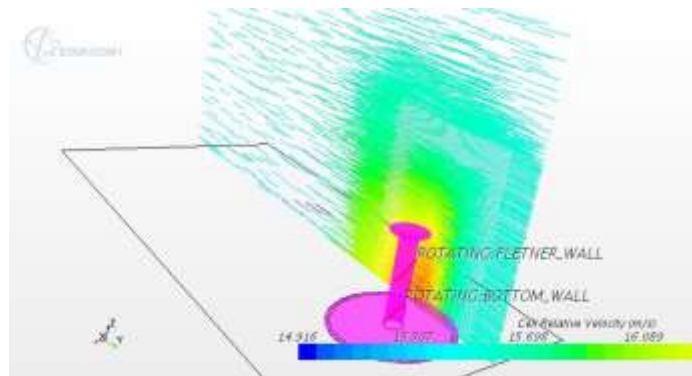


Figure 6: Flow path around the flettner rotor-vector diagram

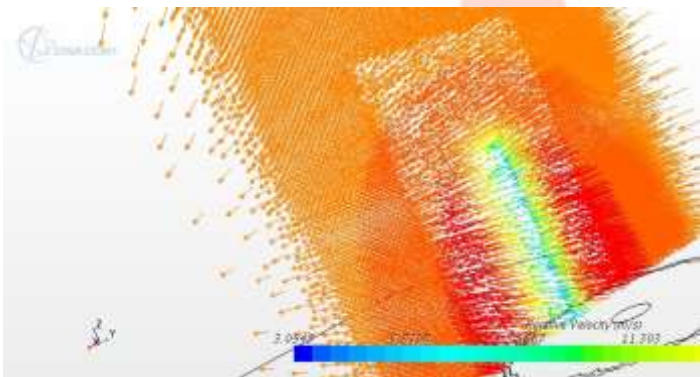


Figure 7: Relative velocity flow path-Vector diagram

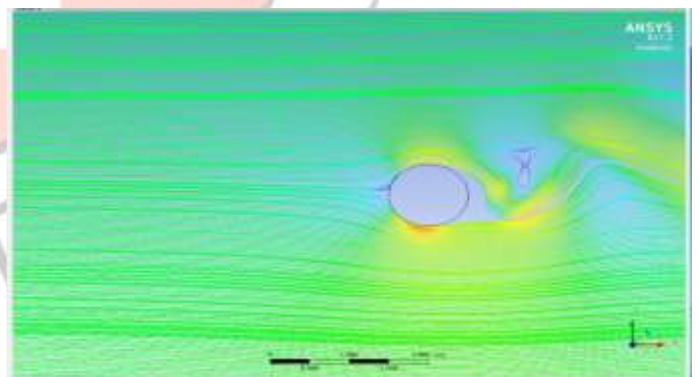


Figure 8: Flow lines-Rotating cylinder at wind speed 15m/s

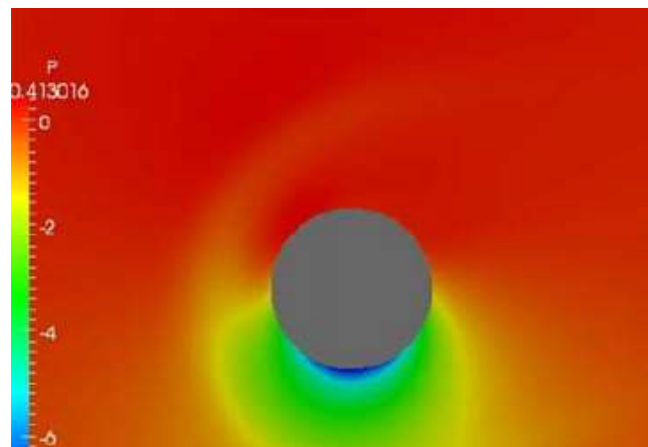


Figure 9: Mean Pressure distribution at the top section

The present study has hopefully advanced our understanding of the performance of the Flettner-rotor driven sea vessels. Nonetheless, a great amount of further investigation is needed to provide more details regarding the following issues. For the case of a smooth cylinder flows, an examination of higher Re flows well within the probably range to be experienced by an actual Flettner-rotor craft is urgent. Examining the flow with a more advanced turbulence model, such as a non-linear eddy-viscosity turbulence model, would deliver more realistic simulations than the linear EVM in the present study. A more complete study for a range of higher spin rates in high Re to understand the reported asymptotic limit in lift previously reported for winds speeds representative of those expected in actual Flettner rotor use.

Lastly, it would be very informative (though numerically challenging) to incorporate an entire rotor within the solution domain to be studied, including end effects (primarily those of a vessel's deck simply modelled by a plane) and the effect of varied wind speed along the length of the cylinder. The proposal of adding discs to gain improvements in rotor aerodynamics must be investigated further. There is a desire to upgrade the near-wall treatment presently covered by wall functions after a study by Zacharos (2010) showed that the flow near a rotating disc surface is largely different if the wall function is modified to allow velocity skewing. With this method, he was able to reproduce the 'Ekman spirals' that form next to spinning discs.

The information provided in the present study and that of Thom (1934) were found to be greatly different and further experimental investigation is needed. Also, a study incorporating further untested geometries with Thom discs would provide a better understanding of the flow behaviour with changes in geometry. A numerical study using LES such as provided by Karabelas (2010) for rotating smooth cylinder flows would be beneficial in a similar study with the addition of Thom discs.

Furthermore, in a comparison effort partnered with the potential smooth cylinder investigation, a study of an entire rotor with Thom discs attached will eventually need to be pursued to understand the effects between adjacent disc cavities as Craft et al. (2011) mentioned that neither a periodic or symmetry boundary conditions applied on the rotor ends was correct. This last development may be in the distant future of Flettner rotor research.

## CONCLUSION

In this paper, the analysis results are based on computational fluid dynamics (CFD). The behavioural study of fluid flow around rotating cylinder and steady cylinder is depicted and are represented on simulated figures. Also the coefficient of lift and drag is determined using CFD. The analysis of the experiments reported, do not give any solutions but contribute to the discussion on the possible benefits of rotor powered ships.

## REFERENCES

- [1] Enercon Wind Company, "Enercon E-ship 1: a wind-hybrid commercial cargo ship," in Proceedings of the 4th Conference on Ship Efficiency, Hamburg, Germany, September 2013.
- [2] E. G. Reid, "Tests of rotating cylinders," Technical Notes NACA 209, 1924.
- [3] J.A. Thom, "Effects of discs on the air forces on a rotating cylinder," Reports & Memoranda 1623, Aerospace Research Council, 1934.
- [4] M. W. Swanson, "The Magnus effect: a summary of investigations to date," Journal of Basic Engineering, vol. 83, no. 3, pp. 461–470, 1961.
- [5] L. Da-Qing, M. Leer-Andersen, and B. Allenstrom, "Performance and vortex formation of Flettner rotors at high Reynolds numbers," in Proceedings of 29th Symposium on Naval Hydrodynamics, Gothenburg, Sweden, August 2012.
- [6] J. Seifert, "A review of the Magnus effect in aeronautics," Progress in Aerospace Sciences, vol. 55, pp. 17–45, 2012.
- [7] S. Mittal and B. Kumar, "Flow past a rotating cylinder," Journal of Fluid Mechanics, vol. 476, pp. 303–334, 2003.
- [8] C. Badalamenti and S. A. Prince, "Vortex shedding from a rotating circular cylinder at moderate subcritical Reynolds numbers and high velocity ratio," in Proceedings of the 26th Congress of International Council of the Aeronautical Sciences (ICAS '08), Anchorage, Alaska, USA, September 2008.
- [9] E. R. Gowree and S. A. Prince, "A computational study of the aerodynamics of a spinning cylinder in a crossflow of high Reynolds number," in Proceedings of the 28th Congress of the International Council of the Aeronautical Sciences (ICAS '12), pp. 1138–1147, Brisbane, Australia, September 2012.
- [10] L. Prandtl, "The Magnus effect and wind-powered ships," Naturwissenschaften, vol. 13, pp. 1787–1806, 1925.
- [11] A. De Marco, S. Mancini, and C. Pensa, "Preliminary analysis for marine application of Flettner rotors," in Proceedings of the 2nd International Symposium on Naval Architecture and Maritime (INT-NAM '14), Istanbul, Turkey, October 2014.
- [12] C. Badalamenti and S. A. Prince, "Effects of endplates on a rotating cylinder in crossflow," in Proceedings of the 26th AIAA Applied Aerodynamics Conference, Honolulu, Hawaii, USA, August 2008.
- [13] N. Thouault, C. Breitsamter, N. A. Adams, J. Seifert, C. Badalamenti, and S. A. Prince, "Numerical analysis of a rotating cylinder with spanwise disks," AIAA Journal, vol. 50, no. 2, pp. 271–283, 2012.
- [14] K. C. Morisseau, "Marine application of magnus effect devices," Naval Engineers Journal, vol. 97, no. 1, pp. 51–57, 1985.
- [15] D. R. Pearson, "The use of flettner rotors in efficient ship design," in Proceedings of the Influence of EEDI on Ship Design Conference, London, UK, September 2014.
- [16] M. Traut, P. Gilbert, C. Walsh et al., "Propulsive power contribution of a kite and a Flettner rotor on selected shipping routes," Applied Energy, vol. 113, pp. 362–372, 2014.
- [17] A. De Marco, S. Mancini, C. Pensa, R. Scognamiglio, and L. Vitiello, "Marine application of flettner rotors: numerical study on a systematic variation of geometric factor by DOE approach," in Proceedings of the 6th International Conference on Computational Methods in Marine Engineering (MARINE '15), vol. 1, Rome, Italy, June 2015.
- [18] CD-Adapco, Star-CCM+ User Guide, 2015.